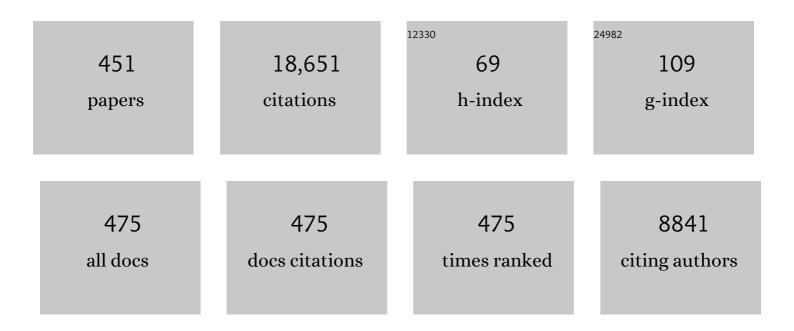
List of Publications by Year in descending order

Source: https://exaly.com/author-pdf/391558/publications.pdf Version: 2024-02-01



ΔΗΤΡΥΟΟΛΝΑΤΗΛΝ

#	Article	IF	CITATIONS
1	Calcific Aortic Valve Disease: Not Simply a Degenerative Process. Circulation, 2011, 124, 1783-1791.	1.6	699
2	Semiautomated method for noise reduction and background phase error correction in MR phase velocity data. Journal of Magnetic Resonance Imaging, 1993, 3, 521-530.	3.4	354
3	Standardized Definition of Structural Valve Degeneration for Surgical and Transcatheter Bioprosthetic Aortic Valves. Circulation, 2018, 137, 388-399.	1.6	350
4	Integrated Mechanism for Functional Mitral Regurgitation. Circulation, 1997, 96, 1826-1834.	1.6	327
5	Fluid Mechanics of Heart Valves. Annual Review of Biomedical Engineering, 2004, 6, 331-362.	12.3	314
6	Heart valve function: a biomechanical perspective. Philosophical Transactions of the Royal Society B: Biological Sciences, 2007, 362, 1369-1391.	4.0	309
7	Review of hydrodynamic principles for the cardiologist: Applications to the study of blood flow and jets by imaging techniques. Journal of the American College of Cardiology, 1988, 12, 1344-1353.	2.8	289
8	Chordal Cutting. Circulation, 2001, 104, 1958-1963.	1.6	285
9	Left ventricular blood flow patterns in normal subjects: A quantitative analysis by three-dimensional magnetic resonance velocity mapping. Journal of the American College of Cardiology, 1995, 26, 224-238.	2.8	243
10	FLUID MECHANICS OF ARTIFICIAL HEART VALVES. Clinical and Experimental Pharmacology and Physiology, 2009, 36, 225-237.	1.9	228
11	Altered Shear Stress Stimulates Upregulation of Endothelial VCAM-1 and ICAM-1 in a BMP-4– and TGF-β1–Dependent Pathway. Arteriosclerosis, Thrombosis, and Vascular Biology, 2009, 29, 254-260.	2.4	212
12	Papillary Muscle Displacement Causes Systolic Anterior Motion of the Mitral Valve. Circulation, 1995, 91, 1189-1195.	1.6	199
13	Elevated cyclic stretch alters matrix remodeling in aortic valve cusps: implications for degenerative aortic valve disease. American Journal of Physiology - Heart and Circulatory Physiology, 2009, 296, H756-H764.	3.2	172
14	Characterization of Hemodynamic Forces Induced by Mechanical Heart Valves: Reynolds vs. Viscous Stresses. Annals of Biomedical Engineering, 2008, 36, 276-297.	2.5	163
15	The Fluid Mechanics of Transcatheter Heart Valve Leaflet Thrombosis in the Neosinus. Circulation, 2017, 136, 1598-1609.	1.6	163
16	Biaixal Stress–Stretch Behavior of the Mitral Valve Anterior Leaflet at Physiologic Strain Rates. Annals of Biomedical Engineering, 2006, 34, 315-325.	2.5	159
17	Nonlinear Power Loss During Exercise in Single-Ventricle Patients After the Fontan. Circulation, 2007, 116, 1165-71.	1.6	157
18	Flow in Prosthetic Heart Valves: State-of-the-Art and Future Directions. Annals of Biomedical Engineering, 2005, 33, 1689-1694.	2.5	155

#	Article	IF	CITATIONS
19	Pressure recovery distal to a stenosis: Potential cause of gradient "verestimation―by Doppler echocardiography. Journal of the American College of Cardiology, 1989, 13, 706-715.	2.8	149
20	Adjacent solid boundaries alter the size of regurgitant jets on Doppler color flow maps. Journal of the American College of Cardiology, 1991, 17, 1094-1102.	2.8	146
21	Elevated Cyclic Stretch Induces Aortic Valve Calcification in a Bone Morphogenic Protein-Dependent Manner. American Journal of Pathology, 2010, 177, 49-57.	3.8	138
22	Hemodynamics and Mechanobiology of Aortic Valve Inflammation and Calcification. International Journal of Inflammation, 2011, 2011, 1-15.	1.5	133
23	Accurate Assessment of Aortic Stenosis. Circulation, 2014, 129, 244-253.	1.6	130
24	In vitro flow experiments for determination of optimal geometry of total cavopulmonary connection for surgical repair of children with functional single ventricle. Journal of the American College of Cardiology, 1996, 27, 1264-1269.	2.8	129
25	In-Vivo Dynamic Deformation of the Mitral Valve Anterior Leaflet. Annals of Thoracic Surgery, 2006, 82, 1369-1377.	1.3	122
26	Endothelium-Dependent Regulation of the Mechanical Properties of Aortic Valve Cusps. Journal of the American College of Cardiology, 2009, 53, 1448-1455.	2.8	122
27	Bileaflet, tilting disc and porcine aortic valve substitutes: In vitro hydrodynamic characteristics. Journal of the American College of Cardiology, 1984, 3, 313-320.	2.8	116
28	Effects of a Saddle Shaped Annulus on Mitral Valve Function and Chordal Force Distribution: An In Vitro Study. Annals of Biomedical Engineering, 2003, 31, 1171-1181.	2.5	115
29	Turbulent shear stress measurements in the vicinity of aortic heart valve prostheses. Journal of Biomechanics, 1986, 19, 433-442.	2.1	112
30	The total cavopulmonary connection resistance: a significant impact on single ventricle hemodynamics at rest and exercise. American Journal of Physiology - Heart and Circulatory Physiology, 2008, 295, H2427-H2435.	3.2	112
31	In Vitro Characterization of the Mechanisms Responsible for Functional Tricuspid Regurgitation. Circulation, 2011, 124, 920-929.	1.6	111
32	An Ex Vivo Study of the Biological Properties of Porcine Aortic Valves in Response to Circumferential Cyclic Stretch. Annals of Biomedical Engineering, 2006, 34, 1655-1665.	2.5	110
33	Mechanism of Mitral Regurgitation in Hypertrophic Cardiomyopathy. Circulation, 1998, 98, 856-865.	1.6	108
34	Toward designing the optimal total cavopulmonary connection: an in vitro study. Annals of Thoracic Surgery, 1999, 68, 1384-1390.	1.3	107
35	Physics-Driven CFD Modeling of Complex Anatomical Cardiovascular Flows?A TCPC Case Study. Annals of Biomedical Engineering, 2005, 33, 284-300.	2.5	106
36	A saddle-shaped annulus reduces systolic strain on the central region of the mitral valve anterior leaflet. Journal of Thoracic and Cardiovascular Surgery, 2007, 134, 1562-1568.	0.8	105

#	Article	IF	CITATIONS
37	Exercise capacity in single-ventricle patients after Fontan correlates with haemodynamic energy loss in TCPC. Heart, 2015, 101, 139-143.	2.9	104
38	Pressure drops across prosthetic aortic heart valves under steady and pulsatile flow—In vitro measurements. Journal of Biomechanics, 1979, 12, 153-164.	2.1	100
39	Flow characteristics of four commonly used mechanical heart valves. American Journal of Cardiology, 1986, 58, 743-752.	1.6	100
40	Clinical significance and origin of artifacts in transesophageal echocardiography of the thoracic aorta. Journal of the American College of Cardiology, 1993, 21, 754-760.	2.8	98
41	Energy loss for evaluating heart valve performance. Journal of Thoracic and Cardiovascular Surgery, 2008, 136, 820-833.	0.8	98
42	Experimental measurement of dynamic fluid shear stress on the aortic surface of the aortic valve leaflet. Biomechanics and Modeling in Mechanobiology, 2012, 11, 171-182.	2.8	97
43	Saddle-Shaped Mitral Valve Annuloplasty Rings Experience Lower Forces Compared With Flat Rings. Circulation, 2008, 118, S250-5.	1.6	96
44	In vitro velocity measurements in the vicinity of aortic prostheses. Journal of Biomechanics, 1979, 12, 135-152.	2.1	94
45	Planar Biaxial Creep and Stress Relaxation of the Mitral Valve Anterior Leaflet. Annals of Biomedical Engineering, 2006, 34, 1509-1518.	2.5	94
46	Introduction of a New Optimized Total Cavopulmonary Connection. Annals of Thoracic Surgery, 2007, 83, 2182-2190.	1.3	94
47	Estimation of the Shear Stress on the Surface of an Aortic Valve Leaflet. Annals of Biomedical Engineering, 1999, 27, 572-579.	2.5	92
48	Evaluation of the Precision of Magnetic Resonance Phase Velocity Mapping for Blood Flow Measurements. Journal of Cardiovascular Magnetic Resonance, 2001, 3, 11-19.	3.3	92
49	Flow in a Mechanical Bileaflet Heart Valve at Laminar and Near-Peak Systole Flow Rates: CFD Simulations and Experiments. Journal of Biomechanical Engineering, 2005, 127, 782-797.	1.3	91
50	Aortic Valve: Mechanical Environment and Mechanobiology. Annals of Biomedical Engineering, 2013, 41, 1331-1346.	2.5	91
51	Fontan hemodynamics: Importance of pulmonary artery diameter. Journal of Thoracic and Cardiovascular Surgery, 2009, 137, 560-564.	0.8	90
52	Mechanistic insights into functional mitral regurgitation. Current Cardiology Reports, 2002, 4, 125-129.	2.9	89
53	Patient-specific surgical planning and hemodynamic computational fluid dynamics optimization through free-form haptic anatomy editing tool (SURGEM). Medical and Biological Engineering and Computing, 2008, 46, 1139-1152.	2.8	88
54	Saddle Shape of the Mitral Annulus Reduces Systolic Strains on the P2 Segment of the Posterior Mitral Leaflet. Annals of Thoracic Surgery, 2009, 88, 1499-1504.	1.3	88

#	Article	IF	CITATIONS
55	Fontan hemodynamics from 100 patient-specific cardiac magnetic resonance studies: A computational fluid dynamics analysis. Journal of Thoracic and Cardiovascular Surgery, 2014, 148, 1481-1489.	0.8	86
56	Mitral valve hemodynamics after repair of acute posterior leaflet prolapse: Quadrangular resection versus triangular resection versus neochordoplasty. Journal of Thoracic and Cardiovascular Surgery, 2009, 138, 309-315.	0.8	81
57	Chordal geometry determines the shape and extent of systolic anterior mitral motion: In vitro studies. Journal of the American College of Cardiology, 1989, 13, 1438-1448.	2.8	80
58	Fluid Dynamic Assessment of Three Polymeric Heart Valves Using Particle Image Velocimetry. Annals of Biomedical Engineering, 2006, 34, 936-952.	2.5	80
59	Coupling Pediatric Ventricle Assist Devices to the Fontan Circulation: Simulations with a Lumped-Parameter Model. ASAIO Journal, 2005, 51, 618-628.	1.6	78
60	Doppler color flow mapping in the evaluation of prosthetic mitral and aortic valve function. Journal of the American College of Cardiology, 1989, 13, 1561-1571.	2.8	75
61	Correction of Pulmonary Arteriovenous Malformation Using Image-Based Surgical Planning. JACC: Cardiovascular Imaging, 2009, 2, 1024-1030.	5.3	75
62	Influence of various instrument settings on the flow information derived from the power mode. Ultrasound in Medicine and Biology, 1991, 17, 49-54.	1.5	74
63	Saddle-shaped mitral valve annuloplasty rings improve leaflet coaptation geometry. Journal of Thoracic and Cardiovascular Surgery, 2011, 142, 697-703.	0.8	74
64	Numerical Simulation of Flow in Mechanical Heart Valves: Grid Resolution and the Assumption of Flow Symmetry. Journal of Biomechanical Engineering, 2003, 125, 709-718.	1.3	73
65	Cyclic Pressure Affects the Biological Properties of Porcine Aortic Valve Leaflets in a Magnitude and Frequency Dependent Manner. Annals of Biomedical Engineering, 2004, 32, 1461-1470.	2.5	73
66	In Vitro Dynamic Strain Behavior of the Mitral Valve Posterior Leaflet. Journal of Biomechanical Engineering, 2005, 127, 504-511.	1.3	73
67	Correlates of Tricuspid Regurgitation as Determined by 3D Echocardiography: Pulmonary Arterial Pressure, Ventricle Geometry, Annular Dilatation, and Papillary Muscle Displacement. Circulation: Cardiovascular Imaging, 2012, 5, 43-50.	2.6	72
68	In Vitro Characterization of Bicuspid Aortic Valve Hemodynamics Using Particle Image Velocimetry. Annals of Biomedical Engineering, 2012, 40, 1760-1775.	2.5	72
69	Chordal force distribution determines systolic mitral leaflet configuration and severity of functional mitral regurgitation. Journal of the American College of Cardiology, 1999, 33, 843-853.	2.8	71
70	Bileaflet, tilting disc and porcine aortic valve substitutes: In vivo hydrodynamic characteristics. Journal of the American College of Cardiology, 1984, 3, 321-327.	2.8	70
71	Three-Dimensional Computational Model of Left Heart Diastolic Function With Fluid–Structure Interaction. Journal of Biomechanical Engineering, 2000, 122, 109-117.	1.3	69
72	On the Mechanics of Transcatheter Aortic Valve Replacement. Annals of Biomedical Engineering, 2017, 45, 310-331.	2.5	69

#	Article	IF	CITATIONS
73	In vitro hemodynamic characteristics of tissue bioprostheses in the aortic position. Journal of Thoracic and Cardiovascular Surgery, 1986, 92, 198-209.	0.8	67
74	Theoretical and practical differences between the Gorlin formula and the continuity equation for calculating aortic and mitral valve areas. American Journal of Cardiology, 1991, 67, 1268-1272.	1.6	67
75	Biosynthetic Activity in Heart Valve Leaflets in Response to In Vitro Flow Environments. Annals of Biomedical Engineering, 2001, 29, 752-763.	2.5	67
76	Total Cavopulmonary Connection Flow With Functional Left Pulmonary Artery Stenosis. Circulation, 2005, 112, 3264-3271.	1.6	67
77	A New Method for Registration-Based Medical Image Interpolation. IEEE Transactions on Medical Imaging, 2008, 27, 370-377.	8.9	67
78	Design of an Ex Vivo Culture System to Investigate the Effects of Shear Stress on Cardiovascular Tissue. Journal of Biomechanical Engineering, 2008, 130, 035001.	1.3	67
79	Experimental measurement of dynamic fluid shear stress on the ventricular surface of the aortic valve leaflet. Biomechanics and Modeling in Mechanobiology, 2012, 11, 231-244.	2.8	67
80	Valve Type, Size, and Deployment Location Affect Hemodynamics in anÂlnÂVitro Valve-in-Valve Model. JACC: Cardiovascular Interventions, 2016, 9, 1618-1628.	2.9	67
81	Slice location dependence of aortic regurgitation measurements with MR phase velocity mapping. Magnetic Resonance in Medicine, 1997, 37, 545-551.	3.0	65
82	Importance of Accurate Geometry in the Study of the Total Cavopulmonary Connection: Computational Simulations and In Vitro Experiments. Annals of Biomedical Engineering, 2001, 29, 844-853.	2.5	65
83	In Vitro Flow Analysis of a Patient-Specific Intraatrial Total Cavopulmonary Connection. Annals of Thoracic Surgery, 2005, 79, 2094-2102.	1.3	64
84	Application of an adaptive control grid interpolation technique to morphological vascular reconstruction. IEEE Transactions on Biomedical Engineering, 2003, 50, 197-206.	4.2	63
85	The material properties of the native porcine mitral valve chordae tendineae: An in vitro investigation. Journal of Biomechanics, 2006, 39, 1129-1135.	2.1	63
86	Dynamic deformation characteristics of porcine aortic valve leaflet under normal and hypertensive conditions. American Journal of Physiology - Heart and Circulatory Physiology, 2010, 298, H395-H405.	3.2	63
87	Mathematics of systolic pulmonary vein flow: A closed form analytical solution incorporating fundamental principles and key variables. Journal of the American College of Cardiology, 1996, 27, 1-2.	2.8	62
88	Functional analysis of Fontan energy dissipation. Journal of Biomechanics, 2008, 41, 2246-2252.	2.1	62
89	Blood flow distribution in a large series of patients having the Fontan operation: A cardiac magnetic resonance velocity mapping study. Journal of Thoracic and Cardiovascular Surgery, 2009, 138, 96-102.	0.8	62
90	An In Vitro Evaluation of the Impact of Eccentric Deployment on Transcatheter Aortic Valve Hemodynamics. Annals of Biomedical Engineering, 2014, 42, 1195-1206.	2.5	61

#	Article	IF	CITATIONS
91	Flow study of an extracardiac connection with persistent left superior vena cava. Journal of Thoracic and Cardiovascular Surgery, 2006, 131, 785-791.	0.8	60
92	On the effects of leaflet microstructure and constitutive model on the closing behavior of the mitral valve. Biomechanics and Modeling in Mechanobiology, 2015, 14, 1281-1302.	2.8	60
93	Geometric Characterization of Patient-Specific Total Cavopulmonary Connections and its Relationship to Hemodynamics. JACC: Cardiovascular Imaging, 2014, 7, 215-224.	5.3	59
94	Determinants of pulmonary venous flow reversal in mitral regurgitation and its usefulness in determining the severity of regurgitation. American Journal of Cardiology, 1999, 83, 535-541.	1.6	58
95	Mitral Valve Function and Chordal Force Distribution Using a Flexible Annulus Model: An In Vitro Study. Annals of Biomedical Engineering, 2005, 33, 557-566.	2.5	58
96	Factors influencing the structure and shape of stenotic and regurgitant jets: An in vitro investigation using doppler color flow mapping and optical flow visualization. Journal of the American College of Cardiology, 1989, 13, 1672-1681.	2.8	55
97	Biofluid Mechanics. , 0, , .		55
98	In vitro pulsatile flow velocity and shear stress measurements in the vicinity of mechanical mitral heart valve prostheses. Journal of Biomechanics, 1986, 19, 39-51.	2.1	54
99	Fluid–Structure Interaction Analysis of Papillary Muscle Forces Using a Comprehensive Mitral Valve Model with 3D Chordal Structure. Annals of Biomedical Engineering, 2016, 44, 942-953.	2.5	54
100	Disturbed Flow Increases UBE2C (Ubiquitin E2 Ligase C) via Loss of miR-483-3p, Inducing Aortic Valve Calcification by the pVHL (von Hippel-Lindau Protein) and HIF-1α (Hypoxia-Inducible Factor-1α) Pathway in Endothelial Cells. Arteriosclerosis, Thrombosis, and Vascular Biology, 2019, 39, 467-481.	2.4	54
101	Experimental and numeric investigation of Impella pumps as cavopulmonary assistance for a failing Fontan. Journal of Thoracic and Cardiovascular Surgery, 2012, 144, 563-569.	0.8	53
102	Pulsatile flow visualization in a model of the human abdominal aorta and aortic bifurcation. Journal of Biomechanics, 1992, 25, 935-944.	2.1	52
103	Computational Modeling of Left Heart Diastolic Function: Examination of Ventricular Dysfunction. Journal of Biomechanical Engineering, 2000, 122, 297-303.	1.3	52
104	Progress in the CFD Modeling of Flow Instabilities in Anatomical Total Cavopulmonary Connections. Annals of Biomedical Engineering, 2007, 35, 1840-1856.	2.5	52
105	Comparing Pre- and Post-operative Fontan Hemodynamic Simulations: Implications for the Reliability of Surgical Planning. Annals of Biomedical Engineering, 2012, 40, 2639-2651.	2.5	52
106	Experimental analysis of fluid mechanical energy losses in aortic valve stenosis: Importance of pressure recovery. Annals of Biomedical Engineering, 1996, 24, 685-694.	2.5	51
107	Cardiac evaluation of women distance runners by echocardiographic color Doppler flow mapping. Journal of the American College of Cardiology, 1988, 11, 89-93.	2.8	50
108	Single-Step Stereolithography of Complex Anatomical Models for Optical Flow Measurements. Journal of Biomechanical Engineering, 2005, 127, 204-207.	1.3	49

#	Article	IF	CITATIONS
109	Structural Characterization of the Chordae Tendineae in Native Porcine Mitral Valves. Annals of Thoracic Surgery, 2005, 80, 189-197.	1.3	49
110	Impaired Power Output and Cardiac Index With Hypoplastic Left Heart Syndrome: A Magnetic Resonance Imaging Study. Annals of Thoracic Surgery, 2006, 82, 1267-1277.	1.3	49
111	Structural simulations of prosthetic tri-leaflet aortic heart valves. Journal of Biomechanics, 2008, 41, 1510-1519.	2.1	49
112	Pulmonary hepatic flow distribution in total cavopulmonary connections: Extracardiac versus intracardiac. Journal of Thoracic and Cardiovascular Surgery, 2011, 141, 207-214.	0.8	49
113	The Effects of Combined Cyclic Stretch and Pressure on the Aortic Valve Interstitial Cell Phenotype. Annals of Biomedical Engineering, 2011, 39, 1654-1667.	2.5	49
114	A Novel Left Heart Simulator for the Multi-modality Characterization of Native Mitral Valve Geometry and Fluid Mechanics. Annals of Biomedical Engineering, 2013, 41, 305-315.	2.5	49
115	New Techniques for the Reconstruction of Complex Vascular Anatomies from MRI Images. Journal of Cardiovascular Magnetic Resonance, 2005, 7, 425-432.	3.3	48
116	Flow simulations in arbitrarily complex cardiovascular anatomies – An unstructured Cartesian grid approach. Computers and Fluids, 2009, 38, 1749-1762.	2.5	48
117	Individualized computer-based surgical planning to address pulmonary arteriovenous malformations in patients with a single ventricle with an interrupted inferior vena cava and azygous continuation. Journal of Thoracic and Cardiovascular Surgery, 2011, 141, 1170-1177.	0.8	48
118	Fluid Mechanic Assessment of the Total Cavopulmonary Connection using Magnetic Resonance Phase Velocity Mapping and Digital Particle Image Velocimetry. Annals of Biomedical Engineering, 2000, 28, 1172-1183.	2.5	47
119	Experimental Investigation of the Steady Flow Downstream of the St. Jude Bileaflet Heart Valve: A Comparison Between Laser Doppler Velocimetry and Particle Image Velocimetry Techniques. Annals of Biomedical Engineering, 2000, 28, 39-47.	2.5	47
120	Numerical, Hydraulic, and Hemolytic Evaluation of an Intravascular Axial Flow Blood Pump to Mechanically Support Fontan Patients. Annals of Biomedical Engineering, 2011, 39, 324-336.	2.5	47
121	A Numerical Investigation of Blood Damage in the Hinge Area of Aortic Bileaflet Mechanical Heart Valves During the Leakage Phase. Annals of Biomedical Engineering, 2012, 40, 1468-1485.	2.5	47
122	Two-dimensional velocity measurements in a pulsatile flow model of the normal abdominal aorta simulating different hemodynamic conditions. Journal of Biomechanics, 1993, 26, 1237-1247.	2.1	46
123	Improved In Vitro Quantification of the Force Exerted by the Papillary Muscle on the Left Ventricular Wall: Three-Dimensional Force Vector Measurement System. Annals of Biomedical Engineering, 2001, 29, 406-413.	2.5	46
124	Effect of Fontan geometry on exercise haemodynamics and its potential implications. Heart, 2017, 103, 1806-1812.	2.9	46
125	Fontan Surgical Planning: Previous Accomplishments, Current Challenges, and Future Directions. Journal of Cardiovascular Translational Research, 2018, 11, 133-144.	2.4	46
126	In vitro methods for studying the accuracy of velocity determination and spatial resolution of a color Doppler flow mapping system. American Heart Journal, 1987, 114, 152-158.	2.7	45

#	Article	IF	CITATIONS
127	Visualization of flow structures in Fontan patients using 3-dimensional phase contrast magnetic resonance imaging. Journal of Thoracic and Cardiovascular Surgery, 2012, 143, 1108-1116.	0.8	45
128	Total ellipse of the heart valve: the impact of eccentric stent distortion on the regional dynamic deformation of pericardial tissue leaflets of a transcatheter aortic valve replacement. Journal of the Royal Society Interface, 2015, 12, 20150737.	3.4	45
129	On the Simulation of Mitral Valve Function in Health, Disease, and Treatment. Journal of Biomechanical Engineering, 2019, 141, .	1.3	45
130	Noninvasive Fluid Dynamic Power Loss Assessments for Total Cavopulmonary Connections Using the Viscous Dissipation Function: A Feasibility Study. Journal of Biomechanical Engineering, 2001, 123, 317-324.	1.3	44
131	Effects of Constant Static Pressure on the Biological Properties of Porcine Aortic Valve Leaflets. Annals of Biomedical Engineering, 2004, 32, 555-562.	2.5	44
132	Effects of Annular Size, Transmitral Pressure, and Mitral Flow Rate on the Edge-To-Edge Repair: An In Vitro Study. Annals of Thoracic Surgery, 2006, 82, 1362-1368.	1.3	44
133	Neonatal Aortic Arch Hemodynamics and Perfusion During Cardiopulmonary Bypass. Journal of Biomechanical Engineering, 2008, 130, 061012.	1.3	44
134	Hemodynamic Modeling of Surgically Repaired Coarctation of the Aorta. Cardiovascular Engineering and Technology, 2011, 2, 288-295.	1.6	44
135	Transcatheter Mitral Valve Planning and the Neo-LVOT: Utilization of Virtual Simulation Models and 3D Printing. Current Treatment Options in Cardiovascular Medicine, 2018, 20, 99.	0.9	44
136	Quantification of mitral regurgitation with MR phase-velocity mapping using a control volume method. Journal of Magnetic Resonance Imaging, 1998, 8, 577-582.	3.4	43
137	In vivo flow dynamics of the total cavopulmonary connection from three-dimensional multislice magnetic resonance imaging. Annals of Thoracic Surgery, 2001, 71, 889-898.	1.3	43
138	Aortic Valve Cyclic Stretch Causes Increased Remodeling Activity and Enhanced Serotonin Receptor Responsiveness. Annals of Thoracic Surgery, 2011, 92, 147-153.	1.3	43
139	The Effects of a Three-Dimensional, Saddle-Shaped Annulus on Anterior and Posterior Leaflet Stretch and Regurgitation of the Tricuspid Valve. Annals of Biomedical Engineering, 2012, 40, 996-1005.	2.5	43
140	Identification of side- and shear-dependent microRNAs regulating porcine aortic valve pathogenesis. Scientific Reports, 2016, 6, 25397.	3.3	43
141	Ex Vivo Methods for Informing Computational Models of the Mitral Valve. Annals of Biomedical Engineering, 2017, 45, 496-507.	2.5	43
142	A New Control Volume Method for Calculating Valvular Regurgitation. Circulation, 1995, 92, 579-586.	1.6	43
143	Two-dimensional mitral flow velocity profiles in pig models using epicardial doppler echocardiography. Journal of the American College of Cardiology, 1994, 24, 532-545.	2.8	42
144	An In Vitro Study of the Hinge and Near-Field Forward Flow Dynamics of the St. Jude Medical® Regentâ,,¢ Bileaflet Mechanical Heart Valve. Annals of Biomedical Engineering, 2000, 28, 524-532.	2.5	42

#	Article	IF	CITATIONS
145	Simulation of the Three-Dimensional Hinge Flow Fields of a Bileaflet Mechanical Heart Valve Under Aortic Conditions. Annals of Biomedical Engineering, 2010, 38, 841-853.	2.5	42
146	Mechanics of the Mitral Valve Strut Chordae Insertion Region. Journal of Biomechanical Engineering, 2010, 132, 081004.	1.3	42
147	Preliminary clinical experience with a bifurcated Y-graft Fontan procedure—A feasibility study. Journal of Thoracic and Cardiovascular Surgery, 2012, 144, 383-389.	0.8	42
148	The Effect of Valve-in-Valve Implantation Height on Sinus Flow. Annals of Biomedical Engineering, 2017, 45, 405-412.	2.5	42
149	Effects of papillary muscle position on in-vitro dynamic strain on the porcine mitral valve. Journal of Heart Valve Disease, 2003, 12, 488-94.	0.5	42
150	Hemodynamic Performance of Stage-2 Univentricular Reconstruction: Glenn vs. Hemi-Fontan Templates. Annals of Biomedical Engineering, 2009, 37, 50-63.	2.5	41
151	Impact of hemodynamics and fluid energetics on liver fibrosis after Fontan operation. Journal of Thoracic and Cardiovascular Surgery, 2018, 156, 267-275.	0.8	41
152	Spatial velocity distribution and acceleration in serial subvalve tunnel and valvular obstructions: An in vitro study using doppler color flow mapping. Journal of the American College of Cardiology, 1989, 13, 241-248.	2.8	40
153	A new theoretical model for noninvasive quantification of mitral regurgitation. Journal of Biomechanics, 1990, 23, 27-33.	2.1	40
154	Miniature C-Shaped Transducers for Chordae Tendineae Force Measurements. Annals of Biomedical Engineering, 2004, 32, 1050-1057.	2.5	40
155	Comparison of the Hinge Flow Fields of Two Bileaflet Mechanical Heart Valves under Aortic and Mitral Conditions. Annals of Biomedical Engineering, 2004, 32, 1607-1617.	2.5	40
156	Cyclic pressure and shear stress regulate matrix metalloproteinases and cathepsin activity in porcine aortic valves. Journal of Heart Valve Disease, 2006, 15, 622-9.	0.5	40
157	A comparison of the hinge and near-hinge flow fields of the St Jude medical hemodynamic plus and regent bileaflet mechanical heart valves. Journal of Thoracic and Cardiovascular Surgery, 2000, 119, 83-93.	0.8	39
158	The Effects of Different Mesh Generation Methods on Computational Fluid Dynamic Analysis and Power Loss Assessment in Total Cavopulmonary Connection. Journal of Biomechanical Engineering, 2004, 126, 594-603.	1.3	39
159	Power loss and right ventricular efficiency in patients after tetralogy of Fallot repair with pulmonary insufficiency: Clinical implications. Journal of Thoracic and Cardiovascular Surgery, 2012, 143, 1279-1285.	0.8	39
160	Simulating hemodynamics of the Fontan Y-graft based on patient-specific inÂvivo connections. Journal of Thoracic and Cardiovascular Surgery, 2013, 145, 663-670.	0.8	39
161	Increased heart rate can cause underestimation of regurgitant jet size by Doppler color flow mapping. Journal of the American College of Cardiology, 1993, 21, 1029-1037.	2.8	38
162	Respiratory Effects on Fontan Circulation During Rest and Exercise Using Real-Time Cardiac Magnetic Resonance Imaging. Annals of Thoracic Surgery, 2016, 101, 1818-1825.	1.3	37

#	Article	IF	CITATIONS
163	Fluid–structure interaction and structural analyses using a comprehensive mitral valve model with 3D chordal structure. International Journal for Numerical Methods in Biomedical Engineering, 2017, 33, e2815.	2.1	37
164	Mitral leaflet geometry perturbations with papillary muscle displacement and annular dilatation: an in-vitro study of ischemic mitral regurgitation. Journal of Heart Valve Disease, 2003, 12, 300-7.	0.5	37
165	In Vitro Mitral Valve Simulator Mimics Systolic Valvular Function of Chronic Ischemic Mitral Regurgitation Ovine Model. Annals of Thoracic Surgery, 2013, 95, 825-830.	1.3	36
166	Bicuspid aortic valves are associated with increased wall and turbulence shear stress levels compared to trileaflet aortic valves. Biomechanics and Modeling in Mechanobiology, 2015, 14, 577-588.	2.8	36
167	Mitral Valve Chordae Tendineae: Topological and Geometrical Characterization. Annals of Biomedical Engineering, 2017, 45, 378-393.	2.5	36
168	Effects of papillary muscle position on chordal force distribution: an in-vitro study. Journal of Heart Valve Disease, 2005, 14, 295-302.	0.5	36
169	Energetic Implications of Vessel Growth and Flow Changes Over Time in Fontan Patients. Annals of Thoracic Surgery, 2015, 99, 163-170.	1.3	35
170	Long-Term Durability of Carpentier-Edwards Magna Ease Valve: A One Billion Cycle InÂVitro Study. Annals of Thoracic Surgery, 2016, 101, 1759-1765.	1.3	35
171	Microflow fields in the hinge region of the CarboMedics bileaflet mechanical heart valve design. Journal of Thoracic and Cardiovascular Surgery, 2002, 124, 561-574.	0.8	34
172	Imaging and patient-specific simulations for the Fontan surgery: Current methodologies and clinical applications. Progress in Pediatric Cardiology, 2010, 30, 31-44.	0.4	34
173	The first cohort of prospective Fontan surgical planning patients with follow-up data: How accurate is surgical planning?. Journal of Thoracic and Cardiovascular Surgery, 2019, 157, 1146-1155.	0.8	34
174	Mechanism of Incomplete Mitral Leaflet Coaptation—Interaction of Chordal Restraint and Changes in Mitral Leaflet Coaptation Geometry. Journal of Biomechanical Engineering, 2002, 124, 596-608.	1.3	33
175	How Can We Help a Patient With a SmallÂFailing Bioprosthesis?. JACC: Cardiovascular Interventions, 2015, 8, 2026-2033.	2.9	33
176	A pulsatile hemodynamic evaluation of the commercially available bifurcated Y-graft Fontan modification and comparison with the lateral tunnel and extracardiac conduits. Journal of Thoracic and Cardiovascular Surgery, 2016, 151, 1529-1536.	0.8	33
177	A Comparison of Flow Field Structures of Two Tri-Leaflet Polymeric Heart Valves. Annals of Biomedical Engineering, 2005, 33, 429-443.	2.5	32
178	Optimum fuzzy filters for phaseâ€contrast magnetic resonance imaging segmentation. Journal of Magnetic Resonance Imaging, 2009, 29, 155-165.	3.4	32
179	Fontan Pathway Growth: A Quantitative Evaluation of Lateral Tunnel and Extracardiac Cavopulmonary Connections Using Serial Cardiac Magnetic Resonance. Annals of Thoracic Surgery, 2014, 97, 916-922.	1.3	32
180	The Advantages of Viscous Dissipation Rate over Simplified Power Loss as a Fontan Hemodynamic Metric. Annals of Biomedical Engineering, 2018, 46, 404-416.	2.5	32

#	Article	IF	CITATIONS
181	Effective Regurgitant Orifice Area by the Color Doppler Flow Convergence Method for Evaluating the Severity of Chronic Aortic Regurgitation. Circulation, 1996, 93, 594-602.	1.6	32
182	Quantifying Aortic Regurgitation by Using the Color Doppler–Imaged Vena Contracta. Circulation, 1997, 96, 2009-2015.	1.6	32
183	Hemodynamic Energy Dissipation in the Cardiovascular System: Generalized Theoretical Analysis on Disease States. Annals of Biomedical Engineering, 2009, 37, 661-673.	2.5	31
184	Numerical Investigation of the Effects of Channel Geometry on Platelet Activation and Blood Damage. Annals of Biomedical Engineering, 2011, 39, 897-910.	2.5	31
185	Right ventricular papillary muscle approximation as a novel technique of valve repair for functional tricuspid regurgitation in an exÂvivo porcine model. Journal of Thoracic and Cardiovascular Surgery, 2012, 144, 235-242.	0.8	31
186	How Local Annular Force and Collagen Density Govern Mitral Annuloplasty Ring Dehiscence Risk. Annals of Thoracic Surgery, 2016, 102, 518-526.	1.3	31
187	Experimental Technique of Measuring Dynamic Fluid Shear Stress on the Aortic Surface of the Aortic Valve Leaflet. Journal of Biomechanical Engineering, 2011, 133, 061007.	1.3	30
188	The congenital bicuspid aortic valve can experience high-frequency unsteady shear stresses on its leaflet surface. American Journal of Physiology - Heart and Circulatory Physiology, 2012, 303, H721-H731.	3.2	30
189	Three-dimensional surface geometry correction is required for calculating flow by the proximal isovelocity surface area technique. Journal of the American Society of Echocardiography, 1995, 8, 585-594.	2.8	29
190	Normal Physiological Conditions Maintain the Biological Characteristics of Porcine Aortic Heart Valves: An Ex Vivo Organ Culture Study. Annals of Biomedical Engineering, 2005, 33, 1158-1166.	2.5	29
191	Quantitative Analysis of Extracardiac Versus Intraatrial Fontan Anatomic Geometries. Annals of Thoracic Surgery, 2008, 85, 810-817.	1.3	29
192	Regional analysis of dynamic deformation characteristics of native aortic valve leaflets. Journal of Biomechanics, 2011, 44, 1459-1465.	2.1	29
193	Clinical Evaluation of New Heart Valve Prostheses: Update of Objective Performance Criteria. Annals of Thoracic Surgery, 2014, 98, 1865-1874.	1.3	29
194	Can time-averaged flow boundary conditions be used to meet the clinical timeline for Fontan surgical planning?. Journal of Biomechanics, 2017, 50, 172-179.	2.1	29
195	Computational Fluid Dynamics Assessment Associated with Transcatheter Heart Valve Prostheses: A Position Paper of the ISO Working Group. Cardiovascular Engineering and Technology, 2018, 9, 289-299.	1.6	29
196	Leg lean mass correlates with exercise systemic output in young Fontan patients. Heart, 2018, 104, 680-684.	2.9	29
197	Chapter 16 Prosthetic Cardiac Valves. Cardiovascular Pathology, 1993, 2, 167-177.	1.6	28
198	Procoagulant Properties of Flow Fields in Stenotic and Expansive Orifices. Annals of Biomedical Engineering, 2008, 36, 1-13.	2.5	28

12

#	Article	IF	CITATIONS
199	High-resolution subject-specific mitral valve imaging and modeling: experimental and computational methods. Biomechanics and Modeling in Mechanobiology, 2016, 15, 1619-1630.	2.8	28
200	In Vitro Fluid Dynamic Characteristics of Ionescu‣hiley and Carpentierâ€Edwards Tissue Bioprostheses. Artificial Organs, 1983, 7, 459-469.	1.9	27
201	A Three-Dimensional Computational Investigation of Intraventricular Fluid Dynamics: Examination Into the Initiation of Systolic Anterior Motion of the Mitral Valve Leaflets. Journal of Biomechanical Engineering, 1995, 117, 94-102.	1.3	27
202	Flow and Thrombosis at Orifices Simulating Mechanical Heart Valve Leakage Regions. Journal of Biomechanical Engineering, 2006, 128, 30-39.	1.3	27
203	Passive flow control of bileaflet mechanical heart valve leakage flow. Journal of Biomechanics, 2008, 41, 1166-1173.	2.1	27
204	What forces act on a flat rigid mitral annuloplasty ring?. Journal of Heart Valve Disease, 2008, 17, 267-75; discussion 275.	0.5	27
205	Design of a Sterile Organ Culture System for the Ex Vivo Study of Aortic Heart Valves. Journal of Biomechanical Engineering, 2005, 127, 857-861.	1.3	26
206	Elevated cyclic stretch and serotonin result in altered aortic valve remodeling via a mechanosensitive 5-HT2A receptor-dependent pathway. Cardiovascular Pathology, 2012, 21, 206-213.	1.6	26
207	Mechanics of Healthy and Functionally Diseased Mitral Valves: A Critical Review. Journal of Biomechanical Engineering, 2013, 135, 021007.	1.3	26
208	Numerical simulation of steady turbulent flow through trileaflet aortic heart valves—II. Results on five models. Journal of Biomechanics, 1985, 18, 909-926.	2.1	25
209	Pulsatile flow velocity and shear stress measurements on the st. jude bileaflet valve prosthesis. Scandinavian Journal of Thoracic and Cardiovascular Surgery, 1986, 20, 15-28.	0.2	25
210	Axial flow velocity patterns in a normal human pulmonary artery model: Pulsatile in vitro studies. Journal of Biomechanics, 1990, 23, 201-214.	2.1	25
211	An Analysis of Turbulent Shear Stresses in Leakage Flow Through a Bileaflet Mechanical Prostheses. Journal of Biomechanical Engineering, 2002, 124, 155-165.	1.3	25
212	An in vitro assessment by means of laser Doppler velocimetry of the medtronic advantage bileaflet mechanical heart valve hinge flow. Journal of Thoracic and Cardiovascular Surgery, 2003, 126, 90-98.	0.8	25
213	Dynamic Hemodynamic Energy Loss in Normal and Stenosed Aortic Valves. Journal of Biomechanical Engineering, 2010, 132, 021005.	1.3	25
214	Fluid-Structure Interaction Analysis of Ruptured Mitral Chordae Tendineae. Annals of Biomedical Engineering, 2017, 45, 619-631.	2.5	25
215	Estimation of Mitral Regurgitation with a Hemielliptic Curve-Fitting Algorithm: In Vitro Experiments with Native Mitral Valvesa~†a~†a~†a~a~a~ Journal of the American Society of Echocardiography, 1998, 11, 3	22-331.	24
216	Bileaflet Aortic Valve Prosthesis Pivot Geometry Influences Platelet Secretion and Anionic Phospholipid Exposure. Annals of Biomedical Engineering, 2001, 29, 657-664.	2.5	24

#	Article	IF	CITATIONS
217	Comparison of Particle Image Velocimetry and Phase Contrast MRI in a Patient-Specific Extracardiac Total Cavopulmonary Connection. Journal of Biomechanical Engineering, 2008, 130, 041004.	1.3	24
218	Dynamic Assessment of Mitral Annular Force Profile in an Ovine Model. Annals of Thoracic Surgery, 2012, 94, 59-65.	1.3	24
219	Imaging for Preintervention Planning. Circulation: Cardiovascular Imaging, 2013, 6, 1092-1101.	2.6	24
220	Valve mediated hemodynamics and their association with distal ascending aortic diameter in bicuspid aortic valve subjects. Journal of Magnetic Resonance Imaging, 2018, 47, 246-254.	3.4	24
221	Analysis of Inlet Velocity Profiles in Numerical Assessment of Fontan Hemodynamics. Annals of Biomedical Engineering, 2019, 47, 2258-2270.	2.5	24
222	Characteristics of surgical prosthetic heart valves and problems around labeling: A document from the European Association for Cardio-Thoracic Surgery (EACTS)—The Society of Thoracic Surgeons (STS)—American Association for Thoracic Surgery (AATS) Valve Labelling Task Force. Journal of Thoracic and Cardiovascular Surgery, 2019, 158, 1041-1054.	0.8	24
223	Development of a Computational Method for Simulating Tricuspid Valve Dynamics. Annals of Biomedical Engineering, 2019, 47, 1422-1434.	2.5	24
224	Comparison of various agents in contrast enhancement of color doppler flow images: An in vitro study. Ultrasound in Medicine and Biology, 1993, 19, 45-57.	1.5	23
225	Three-dimensional reconstruction of the flow in a human left heart by using magnetic resonance phase velocity encoding. Annals of Biomedical Engineering, 1995, 24, 139-147.	2.5	23
226	Assessment of Small-Diameter Aortic Mechanical Prostheses. Circulation, 1998, 98, 866-872.	1.6	23
227	Numerical Investigation of the Performance of Three Hinge Designs of Bileaflet Mechanical Heart Valves. Annals of Biomedical Engineering, 2010, 38, 3295-3310.	2.5	23
228	A new paradigm for obtaining marketing approval for pediatric-sized prosthetic heart valves. Journal of Thoracic and Cardiovascular Surgery, 2013, 146, 879-886.	0.8	23
229	Blood Damage Through a Bileaflet Mechanical Heart Valve: A Quantitative Computational Study Using a Multiscale Suspension Flow Solver. Journal of Biomechanical Engineering, 2014, 136, 101009.	1.3	23
230	Quantitative Evaluation of Annuloplasty on Mitral Valve Chordae Tendineae Forces to Supplement Surgical Planning Model Development. Cardiovascular Engineering and Technology, 2014, 5, 35-43.	1.6	23
231	Computational simulations of flow dynamics and blood damage through a bileaflet mechanical heart valve scaled to pediatric size and flow. Journal of Biomechanics, 2014, 47, 3169-3177.	2.1	23
232	Mitral valve annuloplasty and anterior leaflet augmentation for functional ischemic mitral regurgitation: Quantitative comparison ofÂcoaptation and subvalvular tethering. Journal of Thoracic and Cardiovascular Surgery, 2014, 148, 1688-1693.	0.8	23
233	Influence of Patient-Specific Characteristics on Transcatheter Heart Valve Neo-Sinus Flow: An In Silico Study. Annals of Biomedical Engineering, 2020, 48, 2400-2411.	2.5	23
234	A High-Fidelity and Micro-anatomically Accurate 3D Finite Element Model for Simulations of Functional Mitral Valve. Lecture Notes in Computer Science, 2013, 7945, 416-424.	1.3	23

#	Article	IF	CITATIONS
235	The role of flow stasis in transcatheter aortic valve leaflet thrombosis. Journal of Thoracic and Cardiovascular Surgery, 2022, 164, e105-e117.	0.8	23
236	A Computational Study of a Thin-Walled Three-Dimensional Left Ventricle During Early Systole. Journal of Biomechanical Engineering, 1994, 116, 307-314.	1.3	22
237	Three-Dimensional Velocity Field Reconstruction. Journal of Biomechanical Engineering, 2004, 126, 727-735.	1.3	22
238	In vitro hemodynamic investigation of the embryonic aortic arch at late gestation. Journal of Biomechanics, 2008, 41, 1697-1706.	2.1	22
239	Micro Particle Image Velocimetry Measurements of Steady Diastolic Leakage Flow in the Hinge of a St. Jude Medical® Regentâ,,¢ Mechanical Heart Valve. Annals of Biomedical Engineering, 2014, 42, 526-540.	2.5	22
240	Cardiac Magnetic Resonance–Derived Metrics Are Predictive of Liver Fibrosis in Fontan Patients. Annals of Thoracic Surgery, 2020, 109, 1904-1911.	1.3	22
241	Fluid-Structure Interaction Simulation of an Intra-Atrial Fontan Connection. Biology, 2020, 9, 412.	2.8	22
242	Impact of mitral valve geometry on hemodynamic efficacy of surgical repair in secondary mitral regurgitation. Journal of Heart Valve Disease, 2014, 23, 79-87.	0.5	22
243	Efficacy of the Edge-to-Edge Repair in the Setting of a Dilated Ventricle: An In Vitro Study. Annals of Thoracic Surgery, 2007, 84, 1578-1584.	1.3	21
244	Larger aortic reconstruction corresponds to diminished left pulmonary artery size in patients with single-ventricle physiology. Journal of Thoracic and Cardiovascular Surgery, 2010, 139, 557-561.	0.8	21
245	Aortic Regurgitation Generates a Kinematic Obstruction Which Hinders Left Ventricular Filling. Annals of Biomedical Engineering, 2017, 45, 1305-1314.	2.5	21
246	A multilayered valve leaflet promotes cell-laden collagen type I production and aortic valve hemodynamics. Biomaterials, 2020, 240, 119838.	11.4	21
247	The role of inorganic pyrophosphate in aortic valve calcification. Journal of Heart Valve Disease, 2014, 23, 387-94.	0.5	21
248	Differential immediate-early gene responses to elevated pressure in porcine aortic valve interstitial cells. Journal of Heart Valve Disease, 2006, 15, 34-41; discussion 42.	0.5	21
249	Numerical simulation of steady turbulent flow through trileaflet aortic heart valves—I. Computational scheme and methodology. Journal of Biomechanics, 1985, 18, 899-907.	2.1	20
250	Cardiac motion can alter proximal isovelocity surface area calculations of regurgitant flow. Journal of the American College of Cardiology, 1993, 22, 1730-1737.	2.8	20
251	Dynamics of systolic pulmonary, venous flow in mitral regurgitation: Mathematical modeling of the pulmonary venous system and atrium. Journal of the American Society of Echocardiography, 1995, 8, 631-642.	2.8	20
252	Thrombin formation in vitro in response to shear-induced activation of platelets. Thrombosis Research, 2007, 121, 397-406.	1.7	20

#	Article	IF	CITATIONS
253	Assessment of Current Continuous Hemofiltration Systems and Development of a Novel Accurate Fluid Management System for Use in Extracorporeal Membrane Oxygenation. Journal of Medical Devices, Transactions of the ASME, 2008, 2, .	0.7	20
254	Effect of flow pulsatility on modeling the hemodynamics in the total cavopulmonary connection. Journal of Biomechanics, 2012, 45, 2376-2381.	2.1	20
255	Cardiovascular magnetic resonance compatible physical model of the left ventricle for multi-modality characterization of wall motion and hemodynamics. Journal of Cardiovascular Magnetic Resonance, 2015, 17, 51.	3.3	20
256	Relationship of Single Ventricle Filling and Preload to Total Cavopulmonary Connection Hemodynamics. Annals of Thoracic Surgery, 2015, 99, 911-917.	1.3	20
257	Surgical Planning of the Total Cavopulmonary Connection: Robustness Analysis. Annals of Biomedical Engineering, 2015, 43, 1321-1334.	2.5	20
258	SURGEM: A solid modeling tool for planning and optimizing pediatric heart surgeries. CAD Computer Aided Design, 2016, 70, 3-12.	2.7	20
259	Evaluation of Prosthetic Heart Valves by Doppler Flow Imaging. Echocardiography, 1986, 3, 513-525.	0.9	19
260	Doppler flow velocity mapping in an in vitro model of the normal pulmonary artery. Journal of the American College of Cardiology, 1988, 12, 1366-1376.	2.8	19
261	Flow Characteristics of the St. Jude Prosthetic Valve: An In Vitro and In Vivo Study. Artificial Organs, 1982, 6, 288-294.	1.9	19
262	Experimentally Validated Hemodynamics Simulations of Mechanical Heart Valves in Three Dimensions. Cardiovascular Engineering and Technology, 2012, 3, 88-100.	1.6	19
263	Treatment planning for a TCPC test case: A numerical investigation under rigid and moving wall assumptions. International Journal for Numerical Methods in Biomedical Engineering, 2013, 29, 197-216.	2.1	19
264	Suture Forces in Undersized Mitral Annuloplasty: Novel Device and Measurements. Annals of Thoracic Surgery, 2014, 98, 305-309.	1.3	19
265	Three-dimensional extent of flow stagnation in transcatheter heart valves. Journal of the Royal Society Interface, 2019, 16, 20190063.	3.4	19
266	Y-graft modification to the Fontan procedure: Increasingly balanced flow over time. Journal of Thoracic and Cardiovascular Surgery, 2020, 159, 652-661.	0.8	19
267	An Evaluation of the Influence of Coronary Flow on Transcatheter Heart Valve Neo-Sinus Flow Stasis. Annals of Biomedical Engineering, 2020, 48, 169-180.	2.5	19
268	The Björk – Shiley Aortic Prosthesis: Flow Characteristics of the Present Model vs. The Convexo-Concave Model. Scandinavian Journal of Thoracic and Cardiovascular Surgery, 1980, 14, 1-5.	0.2	18
269	Altered right ventricular papillary muscle position and orientation in patients with a dilated left ventricle. Journal of Thoracic and Cardiovascular Surgery, 2011, 141, 744-749.	0.8	18
270	Neosinus Flow Stasis Correlates With Thrombus Volume Post-TAVR. JACC: Cardiovascular Interventions, 2019, 12, 1288-1290.	2.9	18

#	Article	IF	CITATIONS
271	Transcatheter aortic valve deployment influences neoâ€sinus thrombosis risk: An in vitro flow study. Catheterization and Cardiovascular Interventions, 2020, 95, 1009-1016.	1.7	18
272	Pressure recovery distal to stenoses: Expanding clinical applications of engineering principles. Journal of the American College of Cardiology, 1993, 21, 1026-1028.	2.8	17
273	Cleft closure and undersizing annuloplasty improve mitral repair in atrioventricular canal defects. Journal of Thoracic and Cardiovascular Surgery, 2008, 136, 1243-1249.	0.8	17
274	Comparison of Artificial Neochordae and Native Chordal Transfer in the Repair of a Flail Posterior Mitral Leaflet: An Experimental Study. Annals of Thoracic Surgery, 2013, 95, 629-633.	1.3	17
275	Non-Newtonian Effects on Patient-Specific Modeling of Fontan Hemodynamics. Annals of Biomedical Engineering, 2020, 48, 2204-2217.	2.5	17
276	Effect of hinge gap width on the microflow structures in 27-mm bileaflet mechanical heart valves. Journal of Heart Valve Disease, 2006, 15, 800-8.	0.5	17
277	Effect of Heart Rate on Centerline Velocities of Pulsatile Intracardiac Jets: An In Vitro Study with Laser Doppler Anemometry and Pulsed Doppler Ultrasound. Journal of the American Society of Echocardiography, 1992, 5, 393-404.	2.8	16
278	The importance of slice location on the accuracy of aortic regurgitation measurements with magnetic resonance phase velocity mapping. Annals of Biomedical Engineering, 1997, 25, 644-652.	2.5	16
279	Reduction of Procoagulant Potential of b-Datum Leakage Jet Flow in Bileaflet Mechanical Heart Valves via Application of Vortex Generator Arrays. Journal of Biomechanical Engineering, 2010, 132, 071011.	1.3	16
280	Using a Novel In Vitro Fontan Model and Condition-Specific Real-Time MRI Data to Examine Hemodynamic Effects of Respiration and Exercise. Annals of Biomedical Engineering, 2018, 46, 135-147.	2.5	16
281	Evaluation of eccentric aortic regurgitation by color Doppler jet and color Doppler—imaged vena contracta measurements: An animal study of quantified aortic regurgitation. American Heart Journal, 1996, 132, 796-804.	2.7	15
282	Transapical beating heart cardioscopy technique for off-pump visualization of heart valves. Journal of Thoracic and Cardiovascular Surgery, 2012, 144, 231-234.	0.8	15
283	Hemodynamics of the Boston Scientific Lotusâ,,¢ Valve: An In Vitro Study. Cardiovascular Engineering and Technology, 2013, 4, 427-439.	1.6	15
284	Numerical and experimental investigation of pulsatile hemodynamics in the total cavopulmonary connection. Journal of Biomechanics, 2013, 46, 373-382.	2.1	15
285	Hemodynamic effects of implanting a unidirectional valve in the inferior vena cava of the Fontan circulation pathway: an in vitro investigation. American Journal of Physiology - Heart and Circulatory Physiology, 2013, 305, H1538-H1547.	3.2	15
286	Effect of Hinge Gap Width of a St. Jude Medical Bileaflet Mechanical Heart Valve on Blood Damage Potential—An In Vitro Micro Particle Image Velocimetry Study. Journal of Biomechanical Engineering, 2014, 136, 091008.	1.3	15
287	A Comprehensive Framework for the Characterization of the Complete Mitral Valve Geometry for the Development of a Population-Averaged Model. Lecture Notes in Computer Science, 2015, , 164-171.	1.3	15
288	Suture Dehiscence in the Tricuspid Annulus: An ExÂVivo Analysis of Tissue Strength and Composition. Annals of Thoracic Surgery, 2017, 104, 820-826.	1.3	15

#	Article	IF	CITATIONS
289	Mitral annuloplasty ring suture forces: Impact of surgeon, ring, and use conditions. Journal of Thoracic and Cardiovascular Surgery, 2018, 155, 131-139.e3.	0.8	15
290	Essential information on surgical heart valve characteristics for optimal valve prosthesis selection: expert consensus document from the European Association for Cardio-Thoracic Surgery (EACTS)–The Society of Thoracic Surgeons (STS)–American Association for Thoracic Surgery (AATS)ÀValve Labelling Task Force. European Journal of Cardio-thoracic Surgery, 2021, 59, 54-64.	1.4	15
291	Clinical correlates of the rate of transmission of transmitral "A―wave to the left ventricular outflow tract in left ventricular hypertrophy secondary to systemic hypertension, hypertrophic cardiomyopathy or aortic valve stenosis. American Journal of Cardiology, 1994, 73, 831-834.	1.6	14
292	Modified control grid interpolation for the volumetric reconstruction of fluid flows. Experiments in Fluids, 2008, 45, 987-997.	2.4	14
293	In-vivo transducer to measure dynamic mitral annular forces. Journal of Biomechanics, 2012, 45, 1514-1516.	2.1	14
294	Accuracy of a Mitral Valve Segmentation Method Using J-Splines for Real-Time 3D Echocardiography Data. Annals of Biomedical Engineering, 2013, 41, 1258-1268.	2.5	14
295	Effects of Targeted Papillary Muscle Relocation on Mitral Leaflet Tenting and Coaptation. Annals of Thoracic Surgery, 2013, 95, 621-628.	1.3	14
296	Computational modeling of Fontan physiology: at the crossroads of pediatric cardiology and biomedical engineering. International Journal of Cardiovascular Imaging, 2014, 30, 1073-1084.	1.5	14
297	Personalized mitral valve closure computation and uncertainty analysis from 3D echocardiography. Medical Image Analysis, 2017, 35, 238-249.	11.6	14
298	An inÂvitro analysis of the PediMag and CentriMag for right-sided failing Fontan support. Journal of Thoracic and Cardiovascular Surgery, 2019, 158, 1413-1421.	0.8	14
299	A mechanistic investigation of the EDWARDS INTUITY Elite valve's hemodynamic performance. General Thoracic and Cardiovascular Surgery, 2020, 68, 9-17.	0.9	14
300	Local Hemodynamic Differences Between Commercially Available Y-Grafts and Traditional Fontan Baffles Under Simulated Exercise Conditions: Implications for Exercise Tolerance. Cardiovascular Engineering and Technology, 2017, 8, 390-399.	1.6	14
301	Predictive Model for Thrombus Formation After Transcatheter Valve Replacement. Cardiovascular Engineering and Technology, 2021, 12, 576-588.	1.6	14
302	High Transcatheter Valve Replacement May Reduce Washout in the Aortic Sinuses: an In-Vitro Study. Journal of Heart Valve Disease, 2015, 24, 22-9.	0.5	14
303	Flow Characteristics of Bioprosthetic Heart Valves. Chest, 1990, 98, 365-375.	0.8	13
304	An automated method for analysis and visualization of laser doppler velocimetry data. Annals of Biomedical Engineering, 1997, 25, 335-343.	2.5	13
305	Spatio-temporal Flow Analysis in Bileaflet Heart Valve Hinge Regions: Potential Analysis for Blood Element Damage. Annals of Biomedical Engineering, 2007, 35, 1333-1346.	2.5	13
306	Hemodynamics of the Hepatic Venous Three-Vessel Confluences Using Particle Image Velocimetry. Annals of Biomedical Engineering, 2011, 39, 2398-2416.	2.5	13

#	Article	IF	CITATIONS
307	Cannulation Strategy for Aortic Arch Reconstruction Using Deep Hypothermic Circulatory Arrest. Annals of Thoracic Surgery, 2012, 94, 614-620.	1.3	13
308	Contractile mitral annular forces are reduced with ischemic mitral regurgitation. Journal of Thoracic and Cardiovascular Surgery, 2013, 146, 422-428.	0.8	13
309	Three-Dimensional Field Optimization Method: Gold-Standard Validation of a Novel Color Doppler Method for Quantifying Mitral Regurgitation. Journal of the American Society of Echocardiography, 2016, 29, 917-925.	2.8	13
310	Novel Method to Track Soft Tissue Deformation by Micro-Computed Tomography: Application to the Mitral Valve. Annals of Biomedical Engineering, 2016, 44, 2273-2281.	2.5	13
311	The effect of respiration-driven flow waveforms on hemodynamic metrics used in Fontan surgical planning. Journal of Biomechanics, 2019, 82, 87-95.	2.1	13
312	Effect of Edge-to-Edge Mitral Valve Repair on Chordal Strain: Fluid-Structure Interaction Simulations. Biology, 2020, 9, 173.	2.8	13
313	A three-component force vector cell for in vitro quantification of the force exerted by the papillary muscle on the left ventricular wall. Journal of Biomechanics, 1997, 30, 1071-1075.	2.1	12
314	What Is the Validity of Continuous Wave Doppler Grading of Aortic Regurgitation Severity? A Chronic Animal Model Studyã†ã†ã†ã*:ã*ã* Journal of the American Society of Echocardiography, 1998, 11, 332-337	.2.8	12
315	Evaluation of Cardiovascular Parameters of a Selenium-Based Antihypertensive Using Pulsed Doppler Ultrasound. Journal of Cardiovascular Pharmacology, 2001, 38, 337-346.	1.9	12
316	Laser Flow Measurements in an Idealized Total Cavopulmonary Connection With Mechanical Circulatory Assistance. Artificial Organs, 2011, 35, 1052-1064.	1.9	12
317	Peak Mechanical Loads Induced in the In Vitro Edge-to-Edge Repair of Posterior Leaflet Flail. Annals of Thoracic Surgery, 2012, 94, 1446-1453.	1.3	12
318	Measurement of strut chordal forces of the tricuspid valve using miniature C ring transducers. Journal of Biomechanics, 2012, 45, 1084-1091.	2.1	12
319	Mitral valve annular downsizing forces: Implications for annuloplasty device development. Journal of Thoracic and Cardiovascular Surgery, 2014, 148, 83-89.	0.8	12
320	miR-214 is Stretch-Sensitive in Aortic Valve and Inhibits Aortic Valve Calcification. Annals of Biomedical Engineering, 2019, 47, 1106-1115.	2.5	12
321	Dynamic nature of the LVOT following transcatheter mitral valve replacement with LAMPOON: new insights from post-procedure imaging. European Heart Journal Cardiovascular Imaging, 2022, 23, 650-662.	1.2	12
322	Clinical Impact of Computational Heart Valve Models. Materials, 2022, 15, 3302.	2.9	12
323	Quantitative Approaches to Color Doppler Flow Mapping of Intracardiac Blood Flow: A Review of In Vitro Methods. Echocardiography, 1989, 6, 371-383.	0.9	11
324	Quantification of Cardiac Jets:. Echocardiography, 1994, 11, 267-280.	0.9	11

#	Article	IF	CITATIONS
325	Computational simulations of mitral regurgitation quantification using the flow convergence method: Comparison of hemispheric and hemielliptic formulae. Annals of Biomedical Engineering, 1996, 24, 561-572.	2.5	11
326	Novel method of measuring valvular regurgitation using three-dimensional nonlinear curve fitting of doppler signals within the flow convergence zone. IEEE Transactions on Ultrasonics, Ferroelectrics, and Frequency Control, 2013, 60, 1295-1311.	3.0	11
327	Design of a Pulsatile Flow Facility to Evaluate Thrombogenic Potential of Implantable Cardiac Devices. Journal of Biomechanical Engineering, 2015, 137, 045001.	1.3	11
328	MRI-based Protocol to Characterize the Relationship Between Bicuspid Aortic Valve Morphology and Hemodynamics. Annals of Biomedical Engineering, 2015, 43, 1815-1827.	2.5	11
329	Characterization of aortic root geometry in transcatheter aortic valve replacement patients. Catheterization and Cardiovascular Interventions, 2019, 93, 134-140.	1.7	11
330	Transcatheter aortic valve thrombosis: a review of potential mechanisms. Journal of the Royal Society Interface, 2021, 18, 20210599.	3.4	11
331	The Björk–Shiley Heart Valve Prosthesis.Flow Characteristics of the New 70° Model. Scandinavian Journal of Thoracic and Cardiovascular Surgery, 1982, 16, 1-7.	0.2	10
332	Advances in Cardiovascular Fluid Mechanics: Bench to Bedside. Annals of the New York Academy of Sciences, 2009, 1161, 1-25.	3.8	10
333	Haemodynamic comparison of a novel flow-divider Optiflo geometry and a traditional total cavopulmonary connection. Interactive Cardiovascular and Thoracic Surgery, 2013, 17, 1-7.	1.1	10
334	Comparison of hinge microflow fields of bileaflet mechanical heart valves implanted in different sinus shape and downstream geometry. Computer Methods in Biomechanics and Biomedical Engineering, 2015, 18, 1785-1796.	1.6	10
335	Hemodynamic Impact of Superior Vena Cava Placement in the Y-Graft Fontan Connection. Annals of Thoracic Surgery, 2016, 101, 183-189.	1.3	10
336	In-Vitro Assessment of the Effects of Transcatheter Aortic Valve Leaflet Design on Neo-Sinus Geometry and Flow. Annals of Biomedical Engineering, 2021, 49, 1046-1057.	2.5	10
337	Axial flow velocity patterns in a pulmonary artery model with varying degrees of valvular pulmonic stenosis: Pulsatile in vitro studies. Journal of Biomechanics, 1990, 23, 563-578.	2.1	9
338	Anatomically Realistic Patient-Specific Surgical Planning of Complex Congenital Heart Defects Using MRI and CFD. Annual International Conference of the IEEE Engineering in Medicine and Biology Society, 2007, 2007, 202-5.	0.5	9
339	Uniquely shaped cardiovascular stents enhance the pressure generation of intravascular blood pumps. Journal of Thoracic and Cardiovascular Surgery, 2012, 144, 704-709.	0.8	9
340	Real-time recording of annuloplasty suture dehiscence reveals a potential mechanism for dehiscence cascade. Journal of Thoracic and Cardiovascular Surgery, 2016, 152, e15-e17.	0.8	9
341	Haemodynamic impact of stent implantation for lateral tunnel Fontan stenosis: a patient-specific computational assessment. Cardiology in the Young, 2016, 26, 116-126.	0.8	9
342	A Method for In Vitro TCPC Compliance Verification. Journal of Biomechanical Engineering, 2017, 139, .	1.3	9

#	Article	IF	CITATIONS
343	Mitral annuloplasty ring flexibility preferentially reduces posterior suture forces. Journal of Biomechanics, 2018, 75, 58-66.	2.1	9
344	In Vitro Examination of the VentriFlo True Pulse Pump for Failing Fontan Support. Artificial Organs, 2019, 43, 181-188.	1.9	9
345	Fluid-Structure Interaction Analysis of Subject-Specific Mitral Valve Regurgitation Treatment with an Intra-Valvular Spacer. Prosthesis, 2020, 2, 65-75.	2.9	9
346	Hemodynamic comparison of mitral valve repair: techniques for a flail anterior leaflet. Journal of Heart Valve Disease, 2014, 23, 171-6.	0.5	9
347	An emergency physician's guide to prosthetic heart valves: Identification and hemodynamic function. Annals of Emergency Medicine, 1988, 17, 194-200.	0.6	8
348	Amplitude information from Doppler color flow mapping systems: A preliminary study of the power mode. Journal of the American College of Cardiology, 1991, 18, 997-1003.	2.8	8
349	Temporal Variability of Vena Contracta and Jet Areas with Color Doppler in Aortic Regurgitation: A Chronic Animal Model Study. Journal of the American Society of Echocardiography, 1998, 11, 1064-1071.	2.8	8
350	Comparison by Magnetic Resonance Phase Contrast Imagingof Pulse-Wave Velocity in Patients With Single Ventricle Who Have Reconstructed Aortas Versus Those Without. American Journal of Cardiology, 2014, 114, 1902-1907.	1.6	8
351	Role of Mitral Annulus Diastolic Geometry on Intraventricular Filling Dynamics. Journal of Biomechanical Engineering, 2015, 137, 121007.	1.3	8
352	Isolated effect of geometry on mitral valve function for <i>in silico</i> model development. Computer Methods in Biomechanics and Biomedical Engineering, 2015, 18, 618-627.	1.6	8
353	The hemodynamic effects of acute aortic regurgitation into a stiffened left ventricle resulting from chronic aortic stenosis. American Journal of Physiology - Heart and Circulatory Physiology, 2016, 310, H1801-H1807.	3.2	8
354	Suture dehiscence and collagen content in the human mitral and tricuspid annuli. Biomechanics and Modeling in Mechanobiology, 2019, 18, 291-299.	2.8	8
355	Comparison of Fontan Surgical Options for Patients with Apicocaval Juxtaposition. Pediatric Cardiology, 2020, 41, 1021-1030.	1.3	8
356	Mitral web–a new concept for mitral valve repair: improved engineering design and in-vitro studies. Journal of Heart Valve Disease, 2009, 18, 300-6.	0.5	8
357	Creation of a tricuspid valve regurgitation model from tricuspid annular dilatation using the cardioport video-assisted imaging system. Journal of Heart Valve Disease, 2011, 20, 184-8.	0.5	8
358	In Vitro Fluid Dynamic Characteristics of the Medtronic-Hall Pivoting Disc Heart Valve Prosthesis. Scandinavian Journal of Thoracic and Cardiovascular Surgery, 1982, 16, 235-243.	0.2	7
359	Steady and Pulsatile Flow Studies on a Trileaflet Heart Valve Prosthesis. Scandinavian Journal of Thoracic and Cardiovascular Surgery, 1983, 17, 227-236.	0.2	7
360	Quantification of regurgitant flow through bileaflet heart valve prostheses: Theoretical and in vitro studies. Ultrasound in Medicine and Biology, 1993, 19, 461-468.	1.5	7

#	Article	IF	CITATIONS
361	Atrial inflow can alter regurgitant jet size: In vitro studies. Ultrasound in Medicine and Biology, 1995, 21, 459-469.	1.5	7
362	Impact of Pulmonary Hypertension on Tricuspid Valve Function. Annals of Biomedical Engineering, 2013, 41, 709-724.	2.5	7
363	In-vivo mitral annuloplasty ring transducer: Implications for implantation and annular downsizing. Journal of Biomechanics, 2013, 46, 2550-2553.	2.1	7
364	In vitro assessment of available coaptation area as a novel metric for the quantification of tricuspid valve coaptation. Journal of Biomechanics, 2013, 46, 832-836.	2.1	7
365	Effect of high altitude exposure on the hemodynamics of the bidirectional Glenn physiology: Modeling incremented pulmonary vascular resistance and heart rate. Journal of Biomechanics, 2014, 47, 1846-1852.	2.1	7
366	New mitral annular force transducer optimized to distinguish annular segments and multi-plane forces. Journal of Biomechanics, 2016, 49, 742-748.	2.1	7
367	In Vitro Examination of the HeartWare CircuLite Ventricular Assist Device in the Fontan Connection. ASAIO Journal, 2017, 63, 482-489.	1.6	7
368	Might Coronary Flow Influence Transcatheter Heart Valve Neo-Sinus Thrombosis?. Circulation: Cardiovascular Interventions, 2019, 12, e008005.	3.9	7
369	Tricuspid Valve Annular Mechanics: Interactions with and Implications for Transcatheter Devices. Cardiovascular Engineering and Technology, 2019, 10, 193-204.	1.6	7
370	Outcomes of Single Ventricle Patients Undergoing the Kawashima Procedure: Can We Do Better?. World Journal for Pediatric & Congenital Heart Surgery, 2019, 10, 20-27.	0.8	7
371	Optimized mitral annuloplasty ring design reduces loading in the posterior annulus. Journal of Thoracic and Cardiovascular Surgery, 2020, 159, 1766-1774.e2.	0.8	7
372	InÂvitro evaluation of a new aortic valved conduit. Journal of Thoracic and Cardiovascular Surgery, 2021, 161, 581-590.e6.	0.8	7
373	A Simplified In Silico Model of Left Ventricular Outflow in Patients After Transcatheter Mitral Valve Replacement with Anterior Leaflet Laceration. Annals of Biomedical Engineering, 2021, 49, 1449-1461.	2.5	7
374	An integrated macro/micro approach to evaluating pivot flow within the Medtronic ADVANTAGE bileaflet mechanical heart valve. Journal of Heart Valve Disease, 2003, 12, 503-12.	0.5	7
375	Computational Methods for Fluid-Structure Interaction Simulation of Heart Valves in Patient-Specific Left Heart Anatomies. Fluids, 2022, 7, 94.	1.7	7
376	Color Doppler Assessment of High Flow Velocities Using a New Technology: In Vitro and Clinical Studies. Echocardiography, 1990, 7, 763-769.	0.9	6
377	Revisiting the Gorlin equation for aortic stenosis — Is it correctly used in clinical practice?. International Journal of Cardiology, 2013, 168, 2881-2883.	1.7	6
378	Optimizing hepatic flow distribution with the Fontan Y-graft: Lessons from computational simulations. Journal of Thoracic and Cardiovascular Surgery, 2015, 149, 255-256.	0.8	6

#	Article	IF	CITATIONS
379	Atrial systole enhances intraventricular filling flow propagation during increasing heart rate. Journal of Biomechanics, 2016, 49, 618-623.	2.1	6
380	Long-term durability of a new surgical aortic valve: A 1 billion cycle inÂvitro study. JTCVS Open, 2022, 9, 59-69.	0.5	6
381	Fontan Geometry and Hemodynamics Are Associated With Quality of Life in Adolescents and Young Adults. Annals of Thoracic Surgery, 2022, 114, 841-847.	1.3	6
382	Doppler echocardiographic study of porcine bioprosthetic heart valves in the aortic valve position in patients without evidence of cardiac dysfunction. American Journal of Cardiology, 1991, 67, 611-615.	1.6	5
383	A model based on dimensional analysis for noninvasive quantification of valvular regurgitation under confined and impinging conditions: In vitro pulsatile flow validation. Ultrasound in Medicine and Biology, 1995, 21, 899-911.	1.5	5
384	Validation of Cardiac Output as Reported by a Permanently Implanted Wireless Sensor. Journal of Medical Devices, Transactions of the ASME, 2016, 10, .	0.7	5
385	Flow visualization of the non-parallel jet-vortex interaction. Journal of Visualization, 2018, 21, 533-542.	1.8	5
386	Novel In Vitro Test Systems and Insights for Transcatheter Mitral Valve Design, Part I: Paravalvular Leakage. Annals of Biomedical Engineering, 2019, 47, 381-391.	2.5	5
387	Impact of Free-Breathing Phase-Contrast MRI on Decision-Making in Fontan Surgical Planning. Journal of Cardiovascular Translational Research, 2020, 13, 640-647.	2.4	5
388	Cross-Sectional Magnetic Resonance and Modeling Comparison From Just After Fontan to the Teen Years. Annals of Thoracic Surgery, 2020, 109, 574-582.	1.3	5
389	Hemodynamics of a stenosed aortic valve: Effects of the geometry of the sinuses and the positions of the coronary ostia. International Journal of Mechanical Sciences, 2020, 188, 106015.	6.7	5
390	In Vitro Fluid Dynamics of the St Jude Valve Prosthesis in Steady and Pulsatile Flow. Engineering in Medicine, 1988, 17, 181-187.	0.6	4
391	Assessment of the Accuracy of Color Doppler Flow Mapping By Digital Image Analysis. Echocardiography, 1994, 11, 11-28.	0.9	4
392	Hemodynamic assessment of carbomedics bileaflet heart valves by ultrasound: Studies in the aortic and mitral positions. Ultrasound in Medicine and Biology, 1996, 22, 421-430.	1.5	4
393	Design and validation of a diaphragm pump for pediatric CRRT during ECMO. International Journal of Artificial Organs, 2013, 36, 892-899.	1.4	4
394	Editorial. Cardiovascular Engineering and Technology, 2017, 8, 1-2.	1.6	4
395	Effects of annular contraction on anterior leaflet strain using an in vitro simulator with a dynamically contracting mitral annulus. Journal of Biomechanics, 2018, 66, 51-56.	2.1	4
396	Impact of simulated MitraClip on forward flow obstruction in the setting of mitral leaflet tethering: An in vitro investigation. Catheterization and Cardiovascular Interventions, 2018, 92, 797-807.	1.7	4

#	Article	IF	CITATIONS
397	Novel In Vitro Test Systems and Insights for Transcatheter Mitral Valve Design, Part II: Radial Expansion Forces. Annals of Biomedical Engineering, 2019, 47, 392-402.	2.5	4
398	Computational modeling of a right-sided Fontan assist device: Effectiveness across patient anatomies and cannulations. Journal of Biomechanics, 2020, 109, 109917.	2.1	4
399	Transcatheter Aortic Valve Thrombogenesis: A Foreign Materials Perspective. Cardiovascular Engineering and Technology, 2021, 12, 28-36.	1.6	4
400	PULSATILE FLOW VISUALIZATION STUDIES WITH AORTIC AND MITRAL MECHANICAL VALVE PROSTHESES. Chemical Engineering Communications, 1986, 47, 23-48.	2.6	3
401	A Simplified Model for Fluid Spreading in Composite Web Structures. Textile Reseach Journal, 1990, 60, 23-32.	2.2	3
402	Flow visualization in anatomically accurate, flow-through models of the main pulmonary artery trunk. Cardiology in the Young, 1992, 2, 114-120.	0.8	3
403	Transcatheter aortic valve implantation can potentially impact short-term and long-term functionality: An in vitro study. International Journal of Cardiology, 2014, 172, e421-e422.	1.7	3
404	Does TCPC power loss really affect exercise capacity?. Heart, 2015, 101, 575.2-576.	2.9	3
405	Exercise capacity in the Bidirectional Glenn physiology: Coupling cardiac index, ventricular function and oxygen extraction ratio. Journal of Biomechanics, 2015, 48, 1997-2004.	2.1	3
406	Mechanotransduction in small intestinal submucosa scaffolds: fabrication parameters potentially modulate the shear-induced expression of PECAM-1 and eNOS. Journal of Tissue Engineering and Regenerative Medicine, 2017, 11, 1427-1434.	2.7	3
407	Relationship of Aortic Stiffness to Exercise and Ventricular Volumes in Single Ventricles. Annals of Thoracic Surgery, 2019, 108, 574-580.	1.3	3
408	Framework for Planning TMVR using 3-D Imaging, In Silico Modeling, and Virtual Reality. Structural Heart, 2020, 4, 336-341.	0.6	3
409	A Skeletalized Representation of the Total Cavopulmonary Connection. , 2007, , .		3
410	SETTING STANDARDS: Revised ISO 5840 Series Clarifies Testing, Evaluation Procedures for Cardiac Valves. Biomedical Instrumentation and Technology, 2020, 54, 441-443.	0.4	3
411	Abstract 2207: Significant Impact of the Total Cavopulmonary Connection Resistance on Cardiac Output and Exercise Performance in Single Ventricles. Circulation, 2007, 116, .	1.6	3
412	Gradient and pressure recovery of a self-expandable transcatheter aortic valve depends on ascending aorta size: InÂvitro study. JTCVS Open, 2022, , .	0.5	3
413	A model based on dimensional analysis for non-invasive quantification of valvular regurgitation under confined and impinging conditions. Journal of Biomechanics, 1996, 29, 99-102.	2.1	2
414	Quantification of Mitral and Tricuspid Regurgitation Using Jet Centerline Velocities. Echocardiography, 1996, 13, 357-372.	0.9	2

#	Article	IF	CITATIONS
415	A semi-automated method to quantify left ventricular diastolic inflow propagation by magnetic resonance phase velocity mapping. Journal of Magnetic Resonance Imaging, 1999, 9, 544-551.	3.4	2
416	Magnetic resonance imaging-guided surgical design: can we optimise the Fontan operation?. Cardiology in the Young, 2013, 23, 818-823.	0.8	2
417	Hepatic Venous Blood Flow Distribution in the Total Cavopulmonary Connection: Patient-Specific Anatomical Models. , 2007, , .		2
418	Low and Unsteady Shear Stresses Upregulate Calcification Response of the Aortic Valve Leaflets. , 2011, , ,		2
419	Hemodynamic characterization of calcified stenotic human aortic valves before and after treatment with a novel aortic valve repair system. Journal of Heart Valve Disease, 2004, 13, 582-92; discussion 592.	0.5	2
420	Impact of Anchor Location on Mitral Neochordae Forces: An InÂVitro Study. Annals of Thoracic Surgery, 2022, 113, 1378-1384.	1.3	2
421	Left Ventricular Blood Flow Patterns Assessed by Magnetic Resonance Velocity Mapping in Patients with Ischemic Heart Disease. American Journal of Noninvasive Cardiology, 1994, 8, 317-325.	0.1	1
422	Transesophageal color Doppler evaluation of obstructive lesions using the new "Quasar― technology. Ultrasound in Medicine and Biology, 1995, 21, 1021-1028.	1.5	1
423	How sensitive are jet centerline velocities to an opposing flow? Implications for using the centerline method to quantify regurgitant jet flow. Journal of Biomechanics, 1996, 29, 967-971.	2.1	1
424	Pulsatile Hemodynamics of the Fontan Connection: A Tri-Modal Investigation. , 2011, , .		1
425	Response to Letter Regarding Article, "Accurate Assessment of Aortic Stenosis: A Review of Diagnostic Modalities and Hemodynamics― Circulation, 2014, 130, e135.	1.6	1
426	Fifth Anniversary Editorial. Cardiovascular Engineering and Technology, 2015, 6, 1-1.	1.6	1
427	Mitral annuloplasty ring suture dehiscence: In search of more robust techniques. Journal of Thoracic and Cardiovascular Surgery, 2016, 152, 1640.	0.8	1
428	Measurement Technologies for Heart Valve Function. , 2018, , 115-149.		1
429	Percutaneous DLC-Based Total Cavopulmonary Assist Achieves 96-Hour SurvivalÂinÂLethal Cavopulmonary Failure Sheep. Journal of the American College of Cardiology, 2021, 78, 538-540.	2.8	1
430	An Anterior Anastomosis for the Modified Fontan Connection: A Hemodynamic Analysis. Seminars in Thoracic and Cardiovascular Surgery, 2021, 33, 816-823.	0.6	1
431	Alterations in Tricuspid Valve Mechanics as a Result of Annular Dilatation and Papillary Muscle Displacement: An In Vitro Study. , 2010, , .		1
432	Assessing the Hemodynamic Impact of Anterior Leaflet Laceration in Transcatheter Mitral Valve Replacement: An in silico Study. Frontiers in Cardiovascular Medicine, 0, 9, .	2.4	1

#	Article	IF	CITATIONS
433	Flow characteristics of prosthetic heart valves. International Journal of Cardiovascular Imaging, 1989, 4, 5-8.	0.6	0
434	Modified Lawr-Doppler Anemometer to Study Fluid Flow in Microstructures. Textile Reseach Journal, 1990, 60, 266-276.	2.2	0
435	In Response to "Comparison of Particle Image Velocimetry and Laser Doppler Velocimetry Measurements in Turbulent Fluid Flow―by Wernet et al Annals of Biomedical Engineering, 2000, 28, 1395-1396.	2.5	0
436	Advances in Computational Simulations for Interventional Treatments and Surgical Planning. , 2010, , 343-373.		0
437	Letter regarding the Article by Vismara et al Published in Int J Artif Organs 2011; 34 (4): 383–391. International Journal of Artificial Organs, 2012, 35, 158-159.	1.4	0
438	2012 CVET Reviewers. Cardiovascular Engineering and Technology, 2013, 4, 101-101.	1.6	0
439	Blood Damage Quantification in Cardiovascular Flows Through Medical Devices Using a Novel Suspension Flow Method. Journal of Medical Devices, Transactions of the ASME, 2013, 7, 0409091-409091.	0.7	0
440	Diagnosis of "Paradoxical―Low-Gradient Aortic Stenosis Patients. Journal of the American College of Cardiology, 2013, 62, 2345-2346.	2.8	0
441	Reply to the Editor. Journal of Thoracic and Cardiovascular Surgery, 2014, 148, 1771-1772.	0.8	0
442	Response by Sharma et al to Letter Regarding Article, "The Fluid Mechanics of Transcatheter Heart Valve Leaflet Thrombosis in the Neosinus― Circulation, 2018, 137, 2094-2095.	1.6	0
443	Editorial. Cardiovascular Engineering and Technology, 2019, 10, 395-396.	1.6	0
444	ARE FONTAN HEMODYNAMICS PREDICTIVE OF FUTURE LIVER DISEASE IN FONTAN PATIENTS?. Journal of the American College of Cardiology, 2019, 73, 581.	2.8	0
445	Left ventricular flow in the presence of aortic regurgitation. Journal of Biomechanics, 2019, 87, 211.	2.1	0
446	CORONARY FLOW INFLUENCES TRANSCATHETER AORTIC VALVE LEAFLET THROMBOSIS RISK. Journal of the American College of Cardiology, 2019, 73, 1035.	2.8	0
447	Experimental and Computational Studies of the Aortic Bi-leaflet Mechanical Heart Valve (BMHV) Hemodynamics in an Idealized Left Ventricle. , 2012, , .		0
448	Heart Valve Dynamics. , 2014, , 9-1-9-32.		0
449	Farewell Editorial. Cardiovascular Engineering and Technology, 2020, 11, 605-606.	1.6	0
450	Numerical analysis of the hemodynamic performance of bileaflet mechanical heart valves at different implantation angles. Journal of Heart Valve Disease, 2014, 23, 642-50.	0.5	0

#	Article	IF	CITATIONS
451	Fluid Dynamics of Prosthetic Valves. , 2017, , 433-454.		Ο